Mutation of a single amino acid of pregnane X receptor switches an antagonist to agonist by altering AF-2 helix positioning

Cellular and Molecular Life Sciences

Andrew D. Huber[1,#], William C. Wright[1,2,#], Wenwei Lin[1], Kinjal Majumder[3], Jonathan A. Low[1], Jing Wu[1], Cameron D. Buchman[1], David J. Pintel[3], and Taosheng Chen[1,*]

*Corresponding author; Department of Chemical Biology and Therapeutics, St. Jude Children's Research Hospital, Memphis, TN, 38105, USA; email address: taosheng.chen@stjude.org

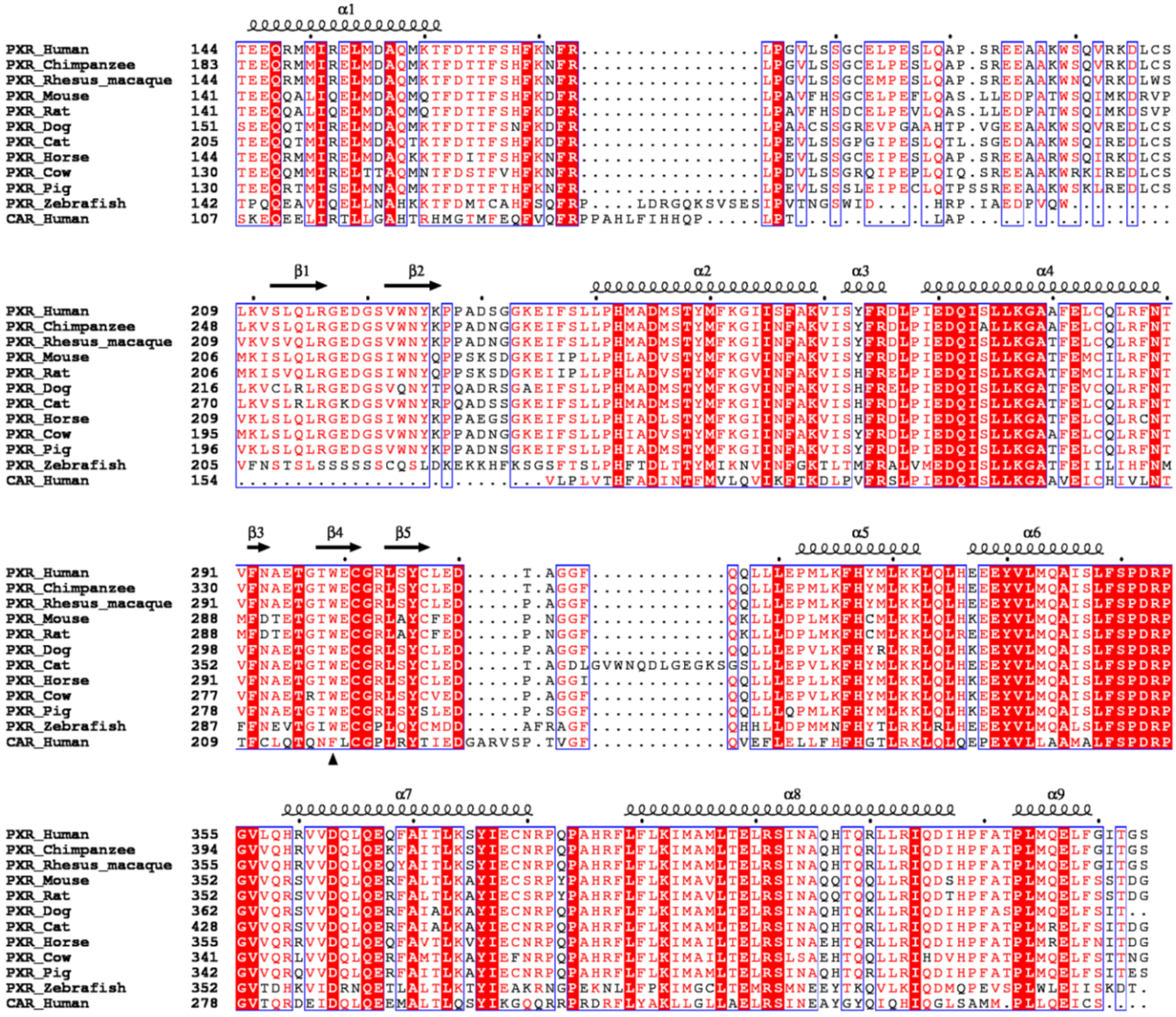

Supplementary Figure 1. Sequence alignments of PXR LBD from multiple species and human CAR LBD. The amino acid sequences of PXR or CAR LBD from the indicated species are aligned and colored by conservation. Secondary structure represents human PXR from PDB 5X0R. The black arrow indicates W299.

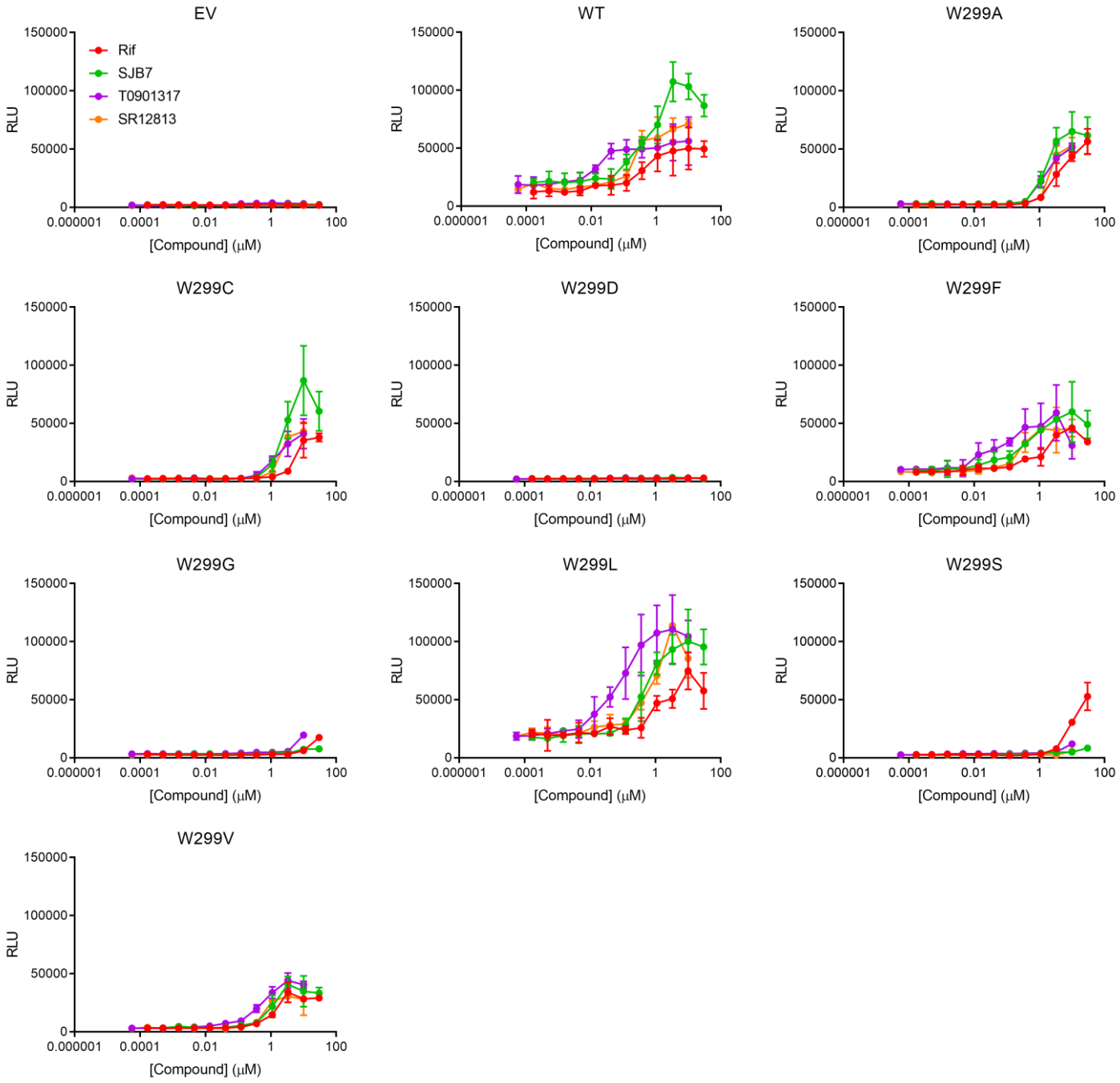

Supplementary Figure 2. Chemical PXR modulation is affected by W299 mutations. HepG2 cells were co-transfected with empty vector (pcDNA3, EV) or wild-type (WT) or W299 mutant PXR-expressing vectors and a plasmid encoding firefly luciferase under the control of a PXR-responsive *CYP3A4* promoter. Cells were treated with the indicated compounds for 24 h and assayed for luciferase activity. RLU, relative light units.

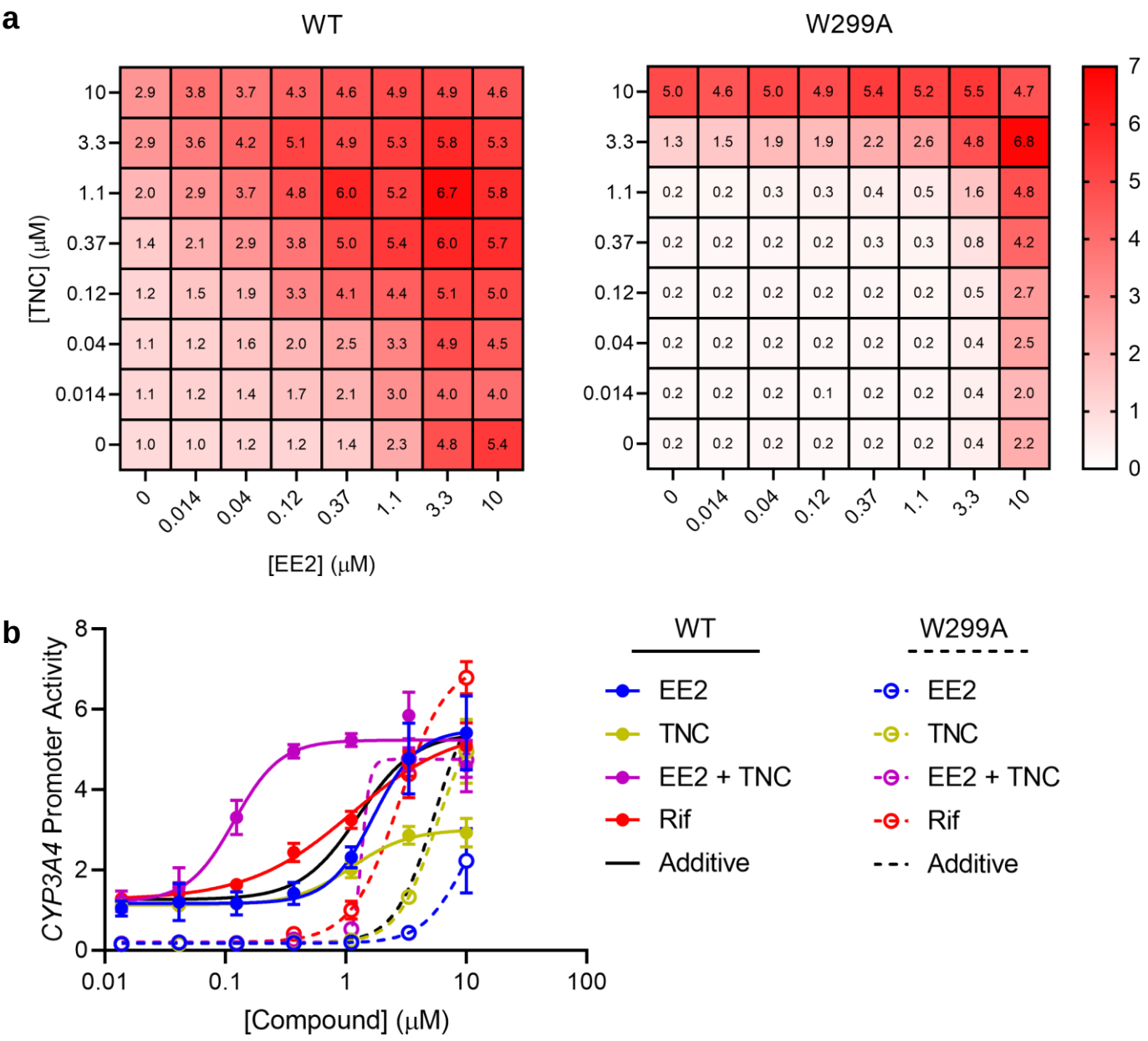

Supplementary Figure 3. W299A reduces TNC and EE2 potency, but retains synergistic activation. HepG2 cells were co-transfected with WT or W299A PXR and a plasmid encoding firefly luciferase under the control of a PXR-responsive *CYP3A4* promoter. Cells were treated with the indicated concentrations of TNC, EE2, or Rif for 24 h and assayed for luciferase activity. (**a**) Heatmaps presented as FC relative to the WT PXR DMSO control. (**b**) Dose response curves derived from (**a**) are shown for Rif alone, EE2 alone, TNC alone, and 1:1 ratios of EE2 + TNC. The black “additive” lines show the theoretical activation curves for the additive combination of EE2 and TNC calculated using the Bliss independence model. Data are presented as fold change relative to the WT PXR DMSO control.

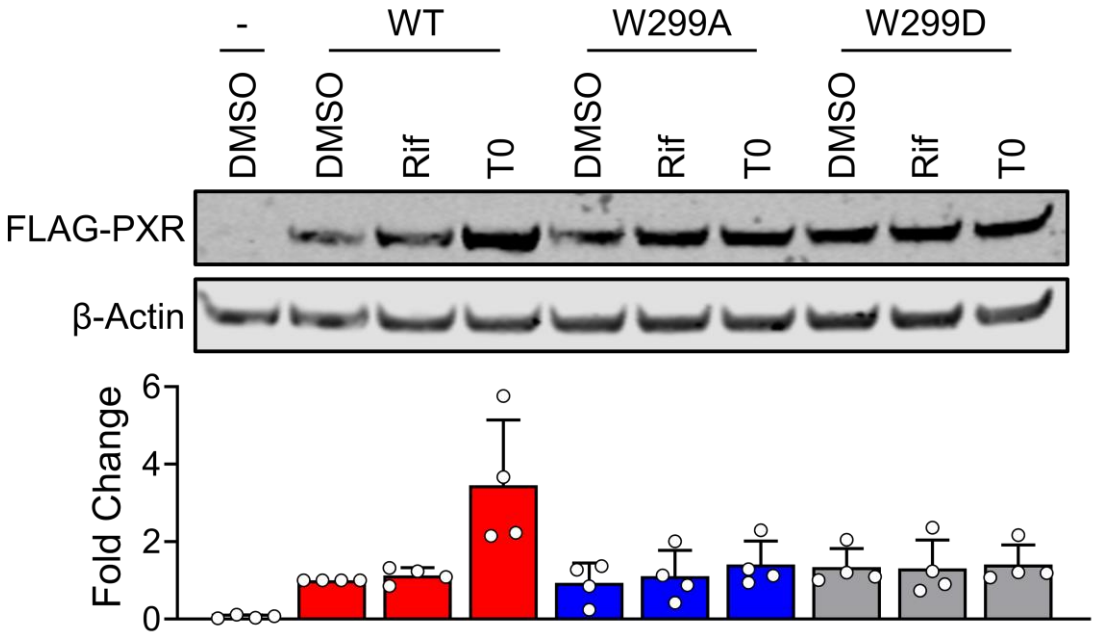

Supplementary Figure 4. Mutation does not affect PXR expression. HepG2 cells were transfected with untagged PXR (-), or FLAG-tagged WT, W299A, or W299D PXR, treated with DMSO, 10 µM Rif, or 5 µM T0, and whole-cell lysates were subjected to western blot after 24 h. The symbols represent measurements from 4 independent experiments. Data are presented as fold change relative to the WT PXR DMSO control.

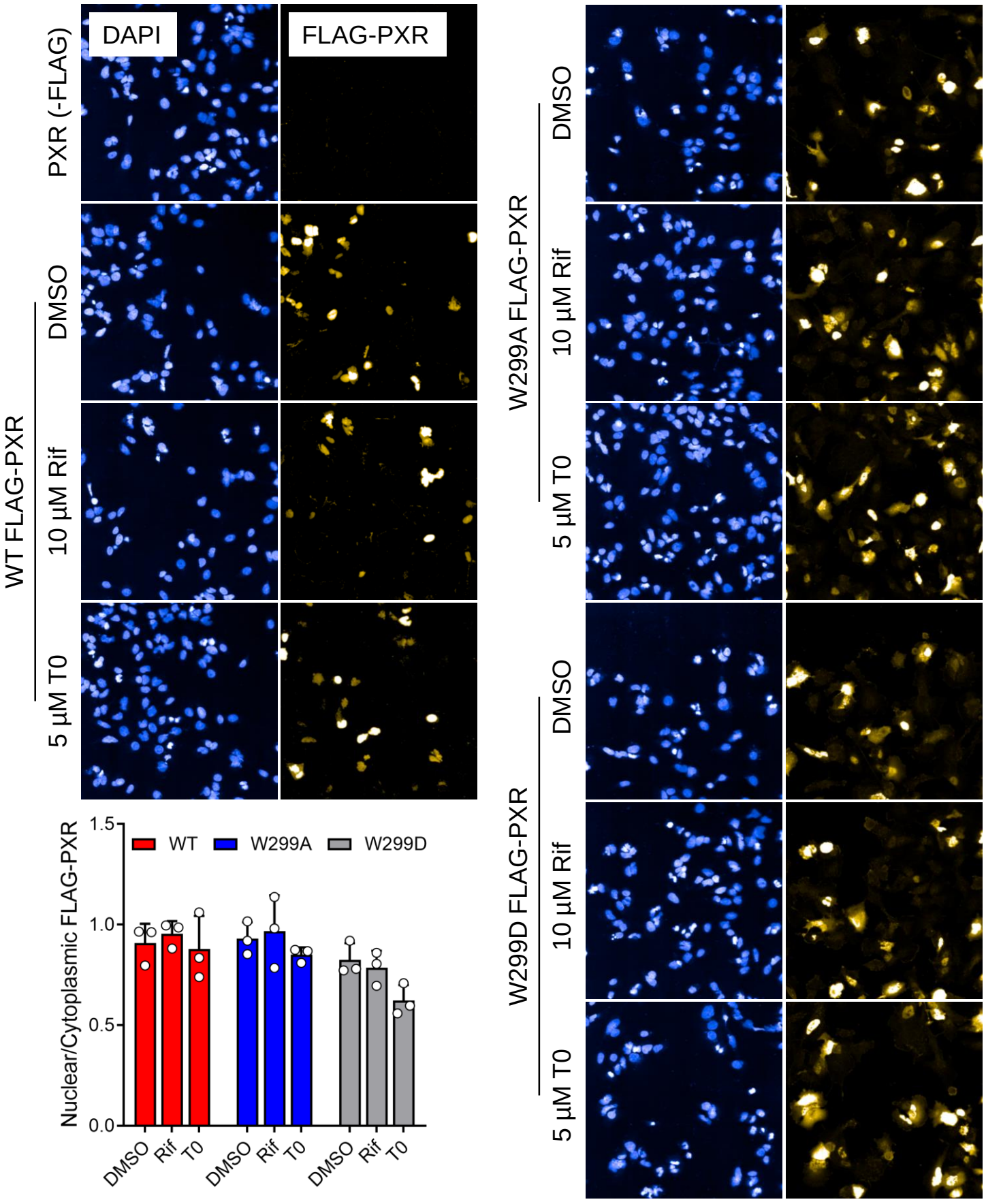

Supplementary Figure 5. Mutant activity differences are not due to localization changes. HepG2 cells were transfected with untagged or FLAG-tagged WT, W299A, or W299D PXR, treated with DMSO, 10 µM Rif or 5 µM T0, and stained with anti-FLAG after 24 h. The ratio of nuclear to cytoplasmic fluorescence was quantified; symbols represent 3 independent experiments.

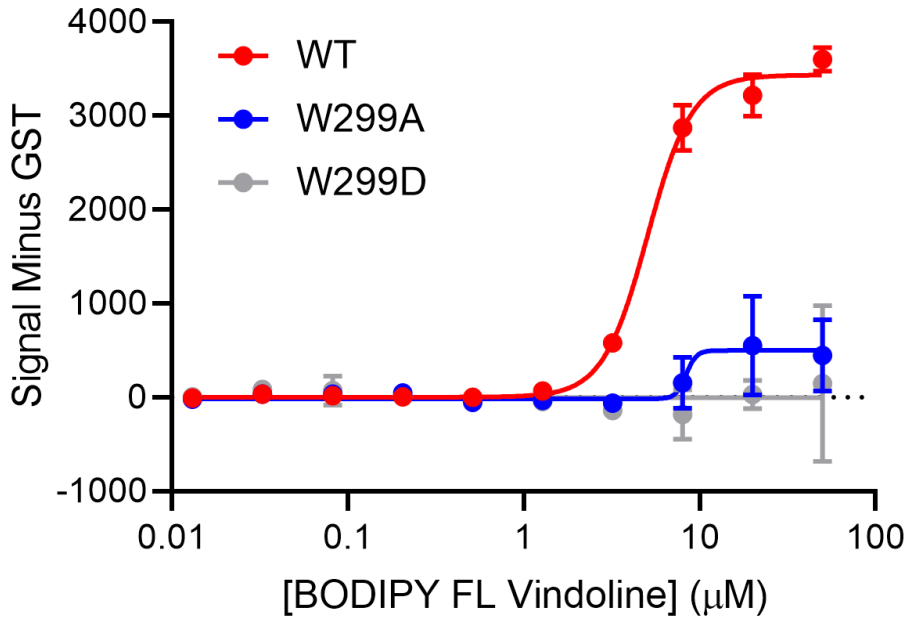

Supplementary Figure 6. W299 mutant PXR has reduced ligand-binding affinity. GST-PXR LBD (WT, W299A, or W299D) or GST alone were produced by *in vitro* transcription/translation, incubated with BODIPY FL vindoline, and TR-FRET signal was measured. The y-axis represents the measured signal minus the corresponding GST signal at each point.

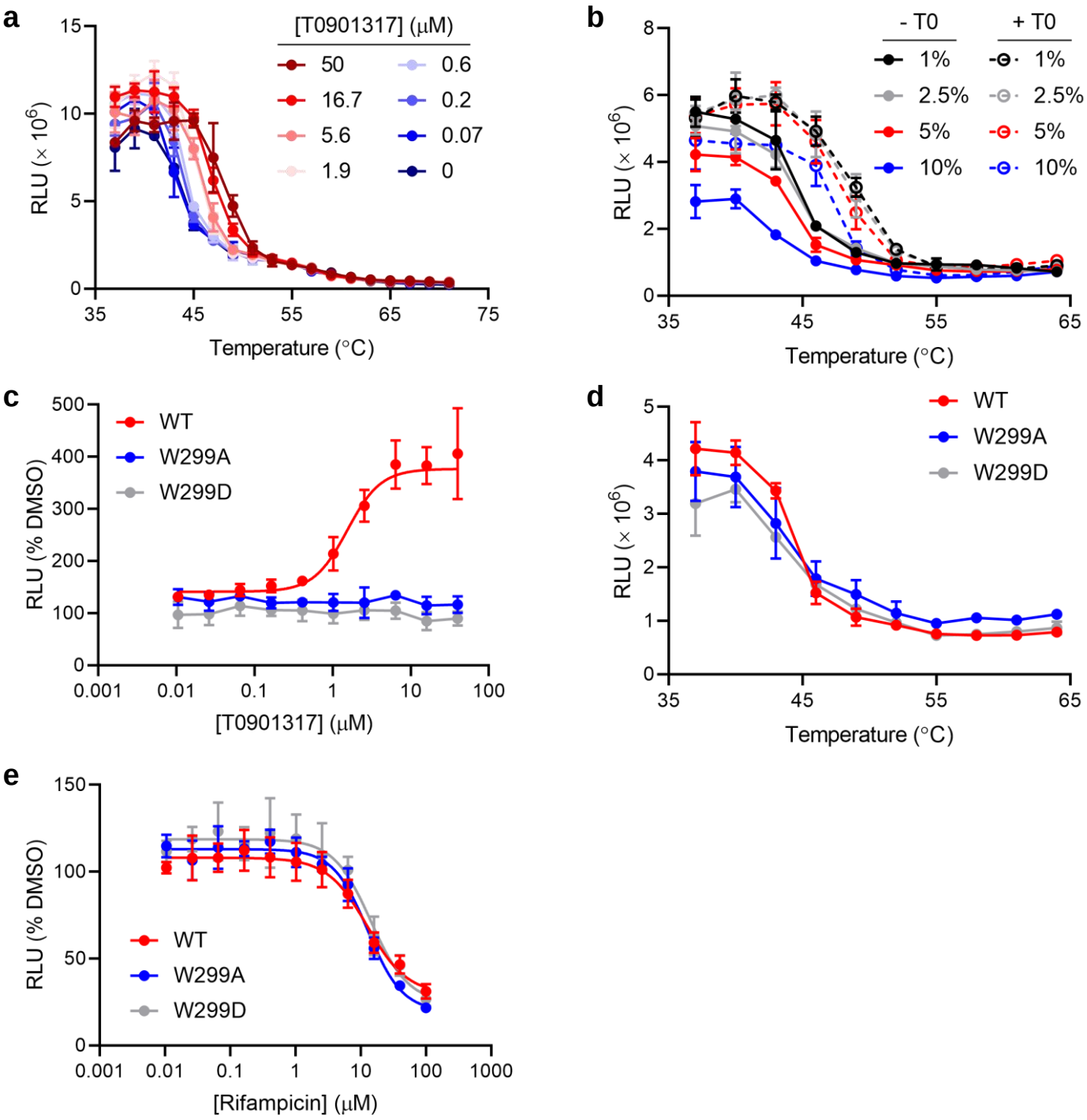

Supplementary Figure 7. W299 mutant PXR has altered T0 binding properties. 293T cells were transfected with the indicated HiBiT-PXR LBD expression vectors, incubated with DMSO or T0 for 1 h at 37°C, and heated in a thermal cycler at the indicated temperatures for 3.5 min. Soluble HiBiT-PXR LBD was measured with the Nano-Glo HiBiT Lytic Detection System (Promega). (**a**) CETSA melting curves for WT HiBiT-tagged PXR LBD with the indicated concentrations of T0. (**b**) CETSA for WT HiBiT-tagged PXR LBD was performed with the indicated concentrations of DMSO in the presence or absence of 50 μM T0. (**c**) CETSA was performed with WT, W299A, and W299D PXR LBD as above, but after 1 h at 37°C, the cells were heated in a thermal cycler at 46°C for 3.5 min. (**d**) CETSA melting curves for WT or mutant HiBiT-tagged PXR LBD with 5% DMSO. (**e**) CETSA was performed with WT, W299A, and W299D PXR LBD with Rif as with T0 in (**c**). RLU, relative light units.

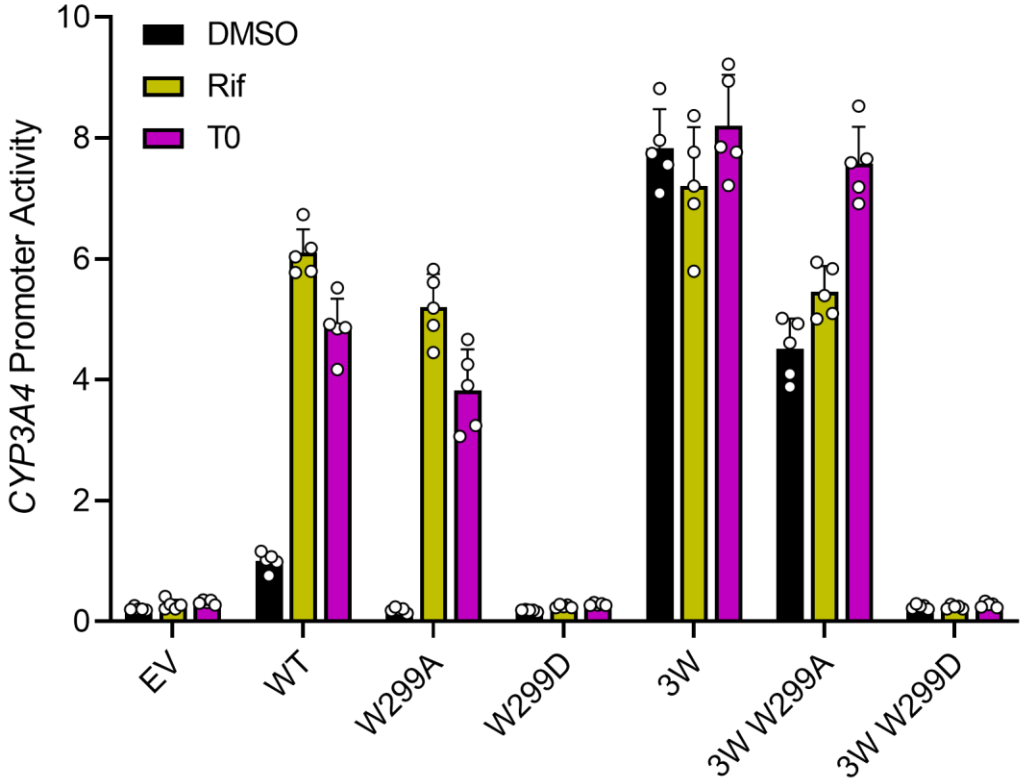

Supplementary Figure 8. The basal activity of W299A PXR is rescued by mutations that mimic ligand binding. HepG2 cells were co-transfected with empty vector (EV) or wild-type (WT) or indicated mutant PXR-expressing vectors and a plasmid encoding firefly luciferase under the control of a PXR-responsive *CYP3A4* promoter. Cells were treated with 10 µM Rif or 5 µM T0 for 24 h and assayed for luciferase activity. Data are presented as fold change relative to the WT PXR DMSO control. Symbols represent 5 independent experiments. 3W has 3 mutations: S208W, S247W, and C284W.

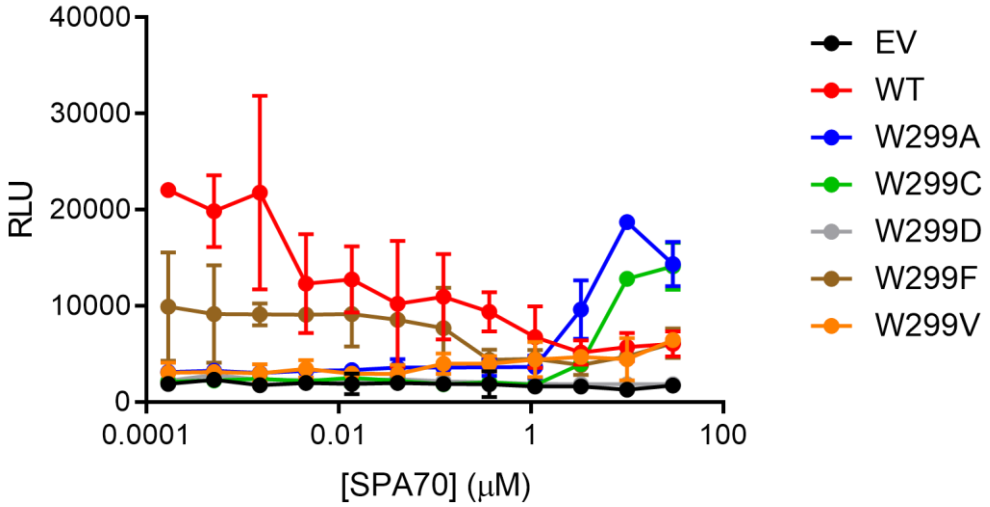

Supplementary Figure 9. PXR modulation by SPA70 is affected by W299 mutations. HepG2 cells were co-transfected with empty vector (pcDNA3, EV) or wild-type (WT) or W299 mutant PXR-expressing vectors and a plasmid encoding firefly luciferase under the control of a PXR-responsive *CYP3A4* promoter. Cells were treated with SPA70 for 24 h and assayed for luciferase activity. RLU, relative light units.

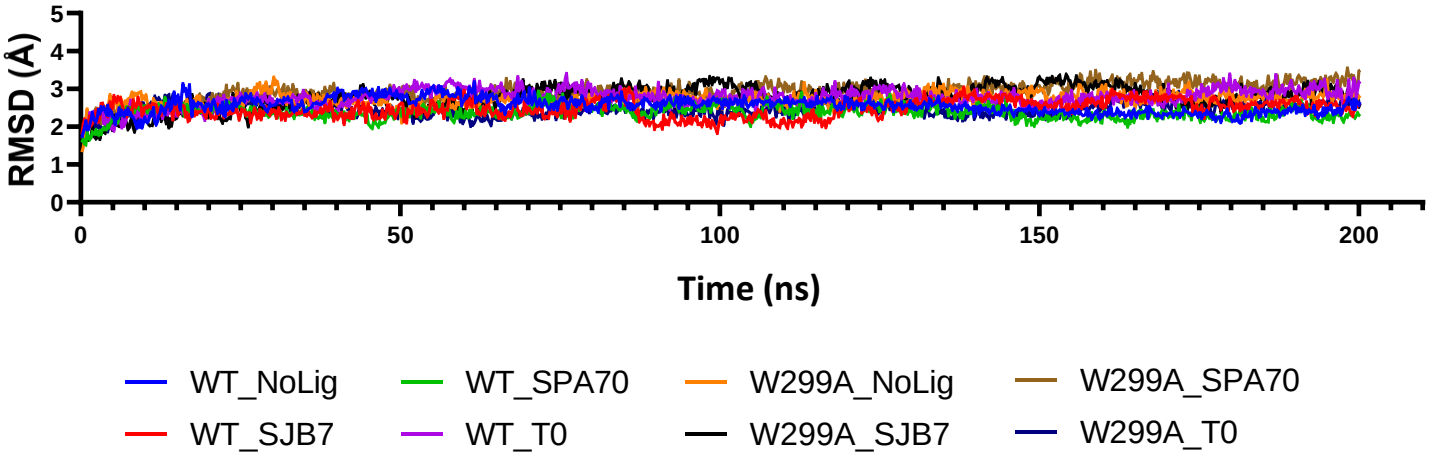

Supplementary Figure 10. MD systems have reached equilibrium. The root mean squared deviation (RMSD) of each system is plotted for the 200 ns simulations.

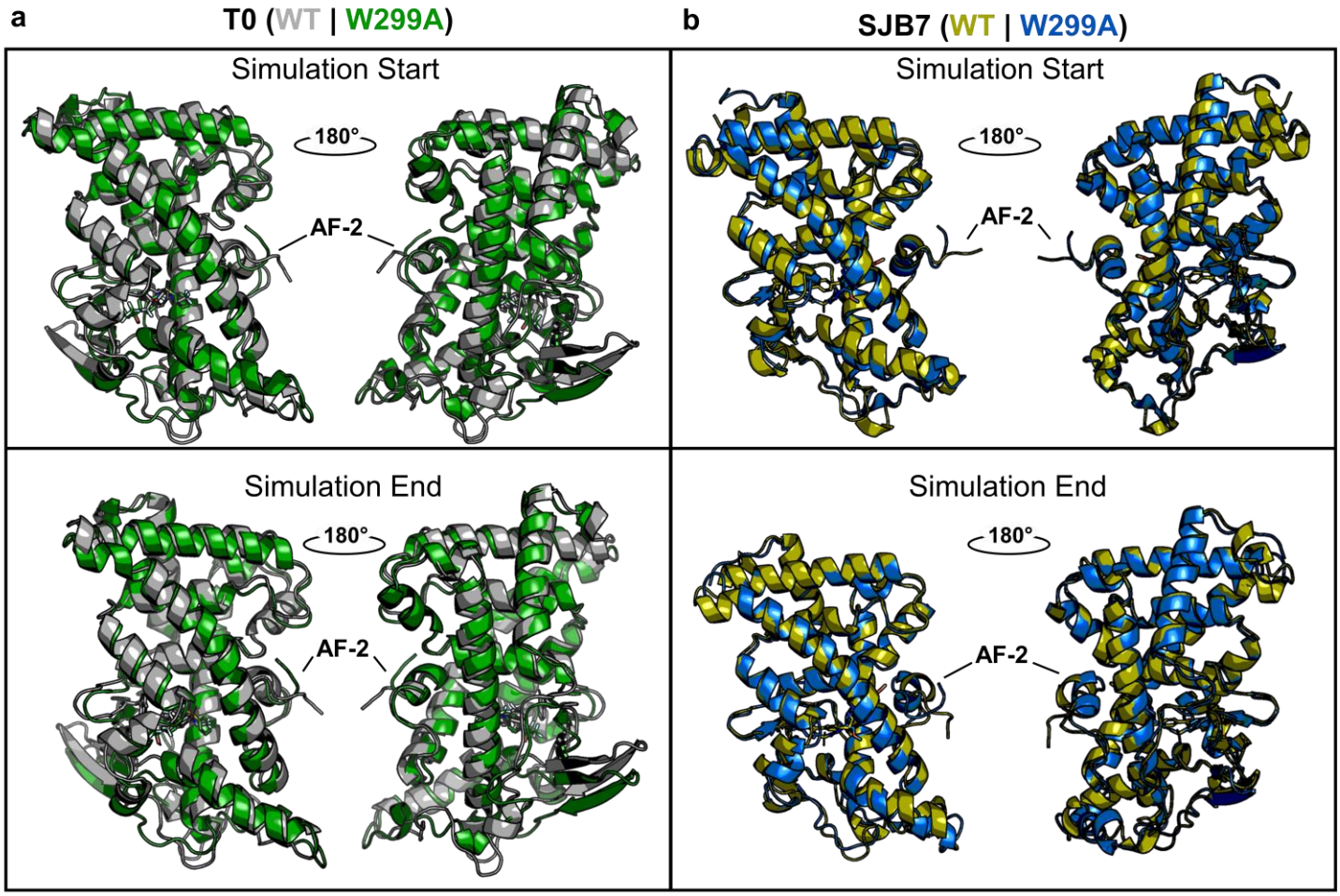

Supplementary Figure 11. There are no significant changes in secondary structures for T0- or SJB7-bound WT or W299A systems over the course of the simulations. (**a**) Overlay of T0-bound WT (gray) or W299A (green) PXR LBD at the beginning (top) and end (bottom) of their respective simulations. (**b**) Overlay of SJB7-bound WT (olive) or W299A (blue) PXR LBD at the beginning (top) and end (bottom) of their respective simulations. Simulation start and end are defined as frame 10 and 1000, respectively.

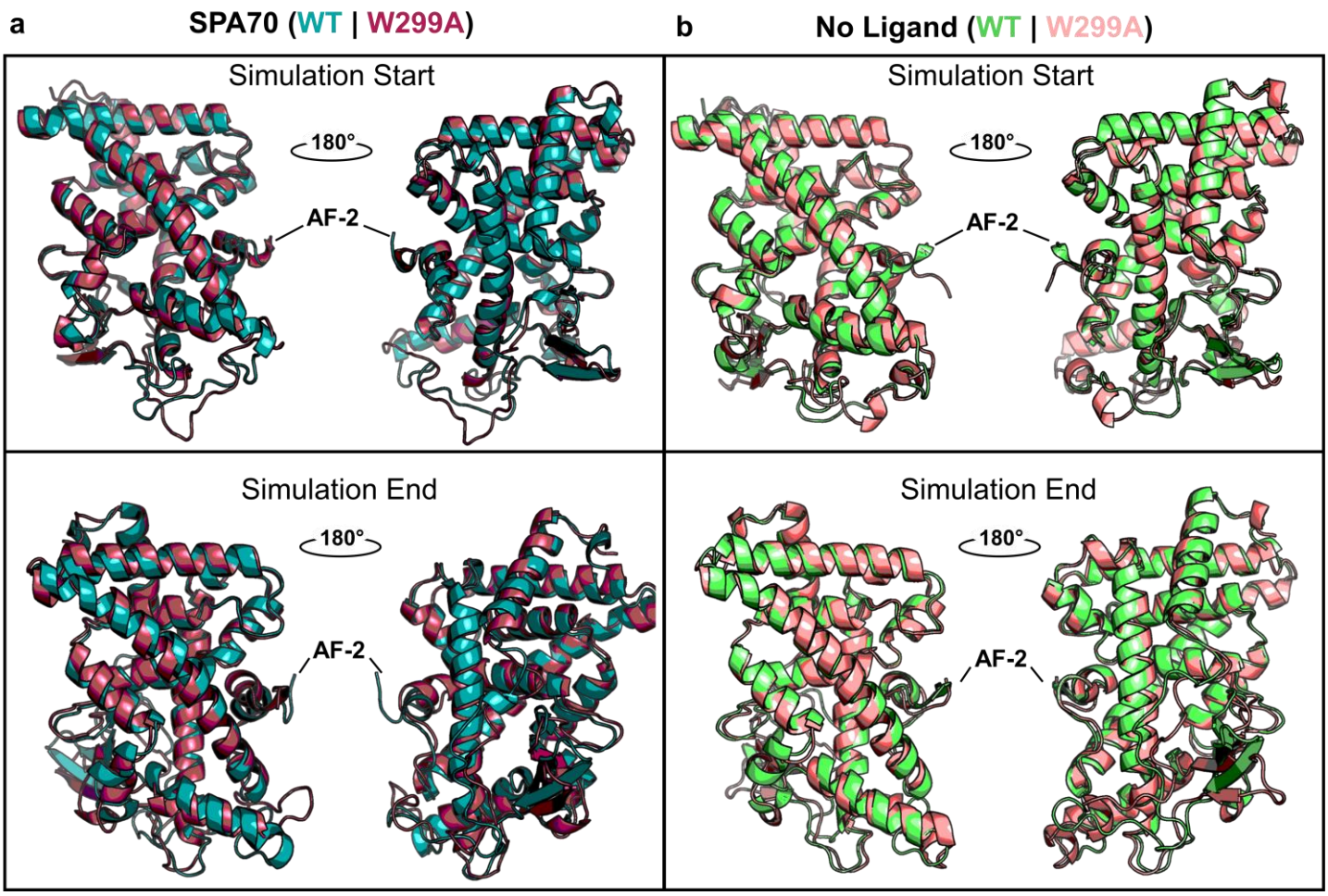

Supplementary Figure 12. PXR LBD W299A mediates AF-2 helix repositioning when bound with SPA70, but confers no change in ligand-free systems. (**a**) Overlay of SPA70-bound WT (teal) or W299A (raspberry) PXR LBD at the beginning (top) and end (bottom) of their respective simulations. (**b**) Overlay of ligand-free WT (lime) or W299A (salmon) PXR LBD at the beginning (top) and end (bottom) of their respective simulations. Simulation start and end are defined as frame 10 and 1000, respectively.

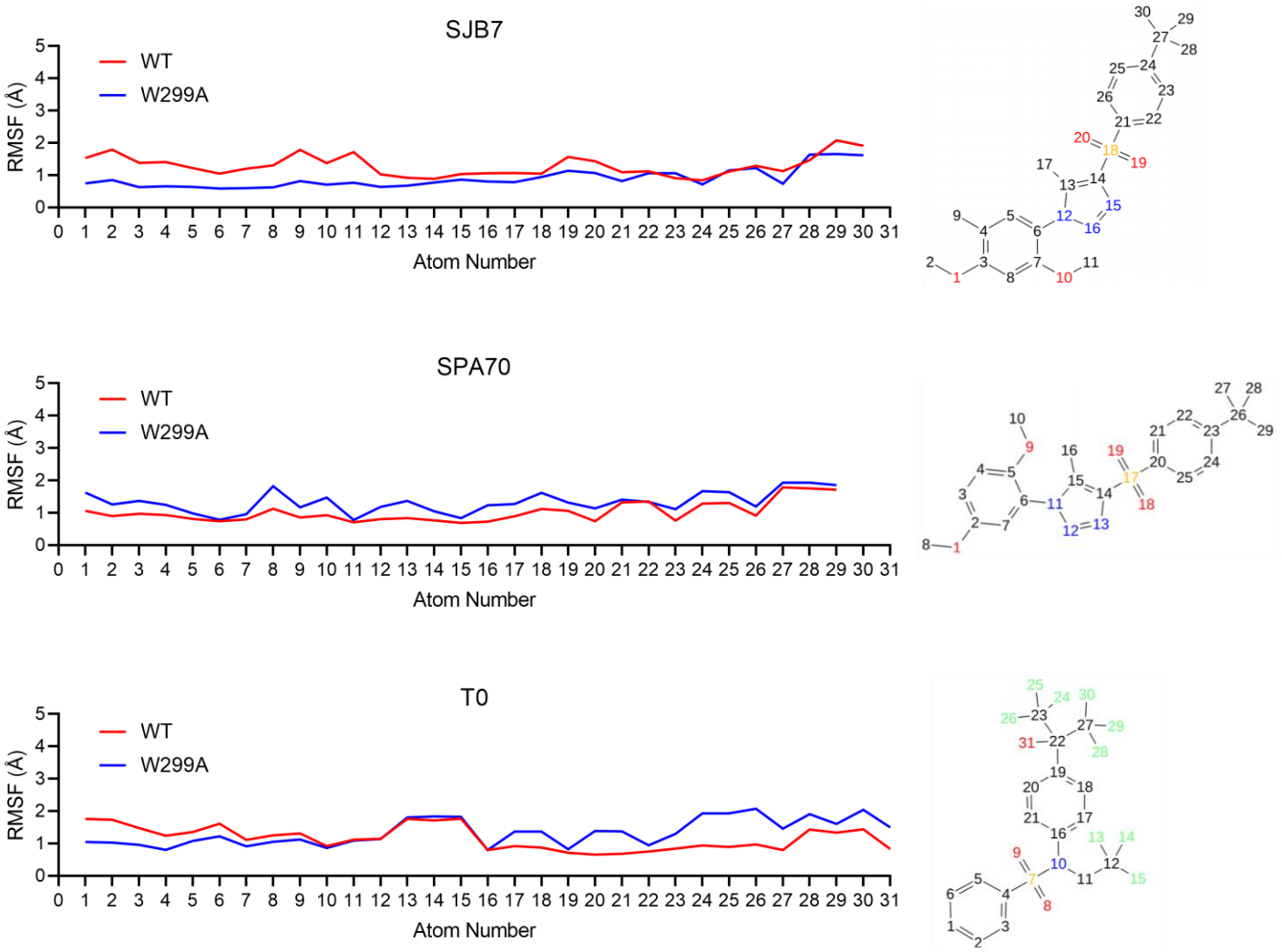

Supplementary Figure 13. The W299A mutation confers no significant changes in ligand stability for SJB7, SPA70, or T0. Overlay of WT and W299A root mean square fluctuation (RMSF) measurements for SJB7, SPA70, and T0. Each x-axis corresponds to the atom numbers of the 2D ligand representations to the right of its respective plot.

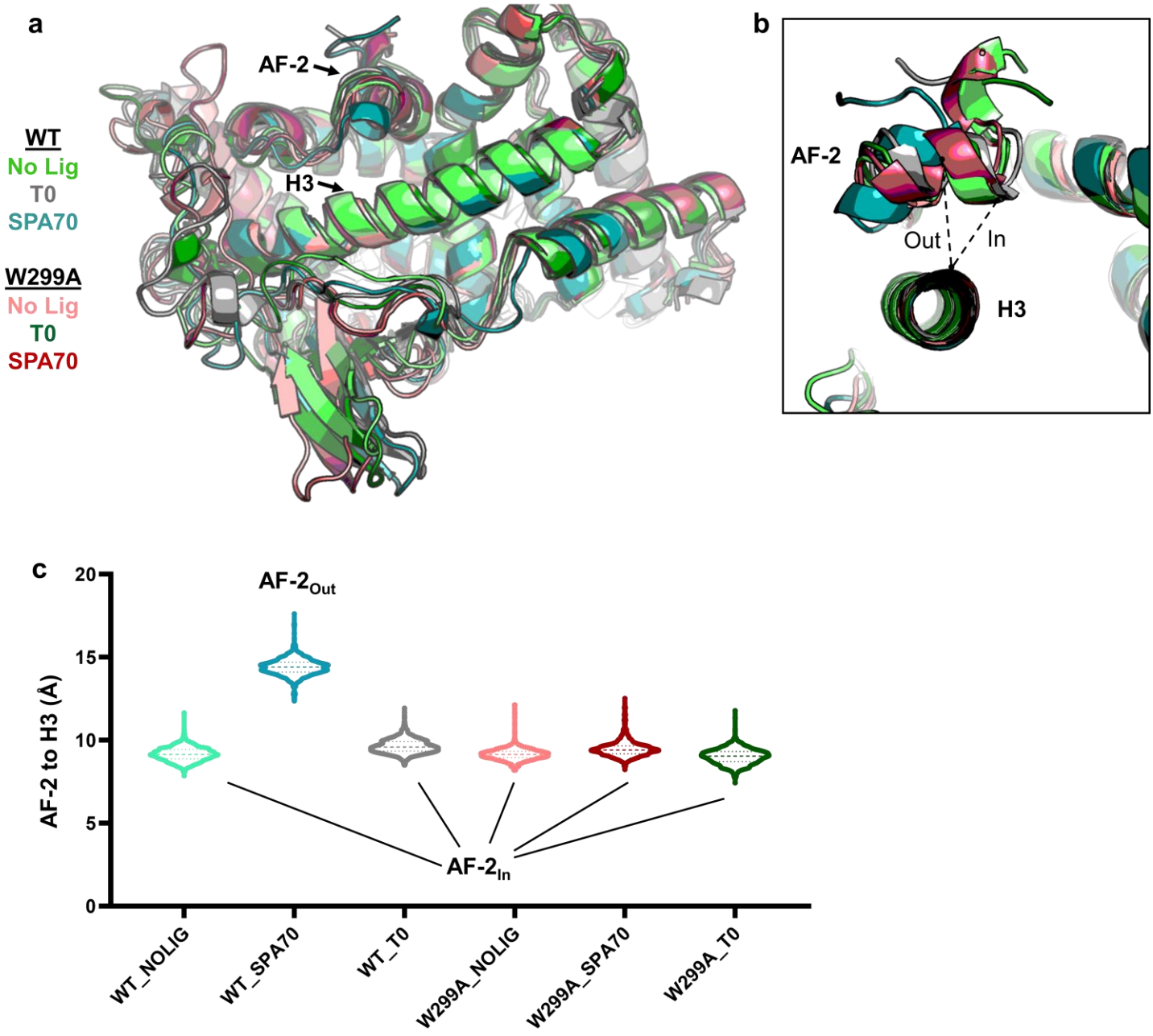

Supplementary Figure 14. SPA70-bound WT PXR LBD mediates AF-2 repositioning, which is lost in the W299A mutant. (**a**) Overlay of ligand-free WT (lime), T0-bound WT (gray), SPA70-bound WT (teal), ligand-free W299A (salmon), T0-bound W299A (green), and SPA70-bound W299A (raspberry) PXR LBD showing the preserved secondary structure of helix 3 (H3). (**b**) The same overlaid structures as (**a**), showing the AF-2 helix as "In" or "Out" with respect to H3. For "In" *vs*. "Out" quantification, the same residue of the AF-2 (F429) was measured to the same conserved reference point on H3 (F251). (**c**) Violin plot of the AF-2 to H3 distance described in (**b**). Quartiles are shown in thin dashed lines, and the medians are shown as thick dashed lines.

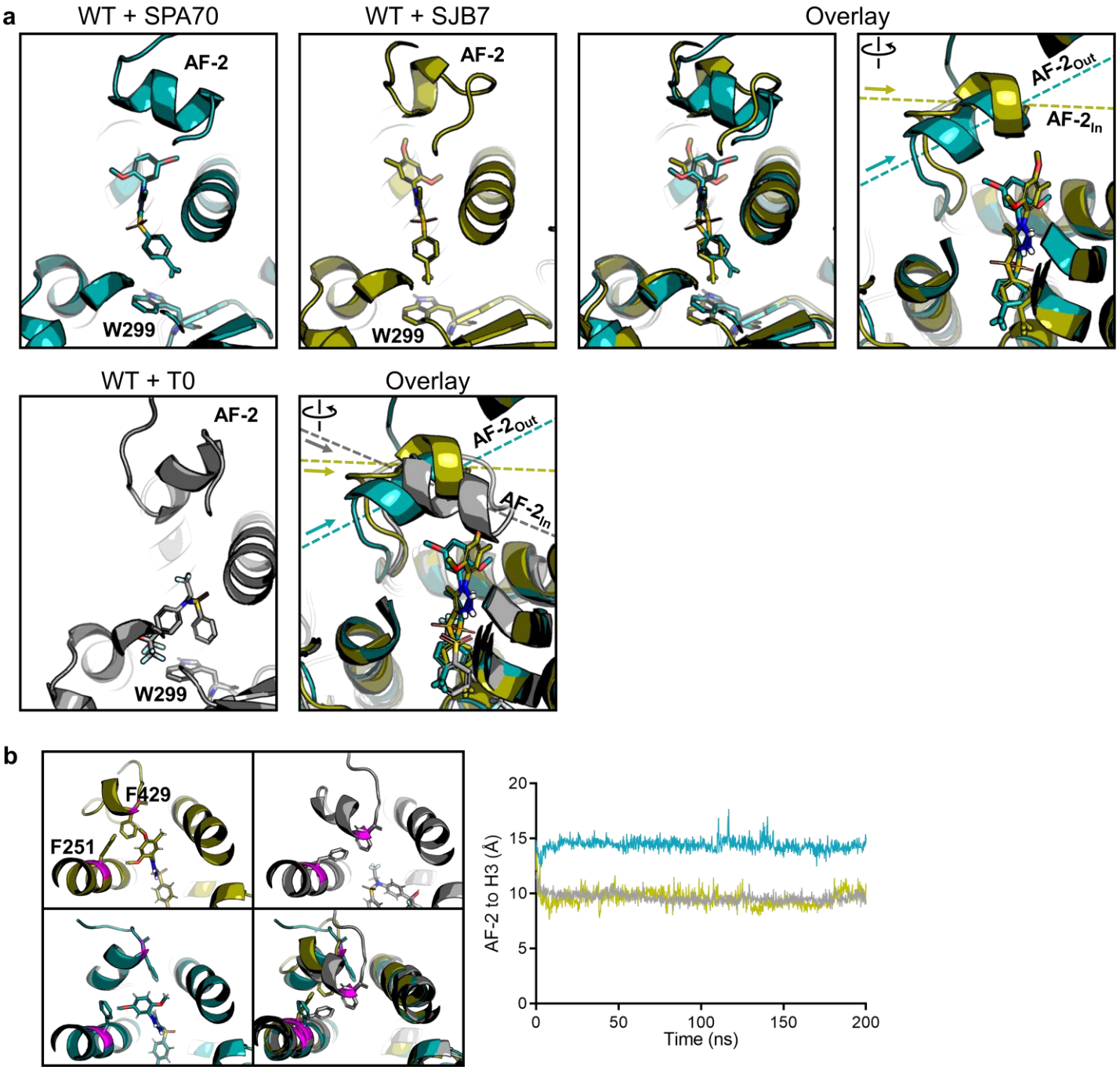

Supplementary Figure 15. SJB7 induces the AF-2$_{In}$ conformation. (**a**) Individual and superimposed images are shown for SPA70-bound (teal), SJB7-bound (olive), and T0-bound (gray) WT PXR LBD. The dashed lines indicate the orientation of each AF-2 helix; arrows point from the N- to the C-terminus of the helix. The AF-2 is labeled “In” or “Out” in reference to the proximity of the C-terminus to the ligand-binding pocket. (**b**) Quantification of the “In” *vs*. “Out” AF-2 orientations between simulations. The distance from the AF-2 residue F429 to the helix 3 residue F251 was measured for the duration of each simulation (using α-carbon atoms for measurements). The α-carbons of the residues used for quantification are shown in magenta.

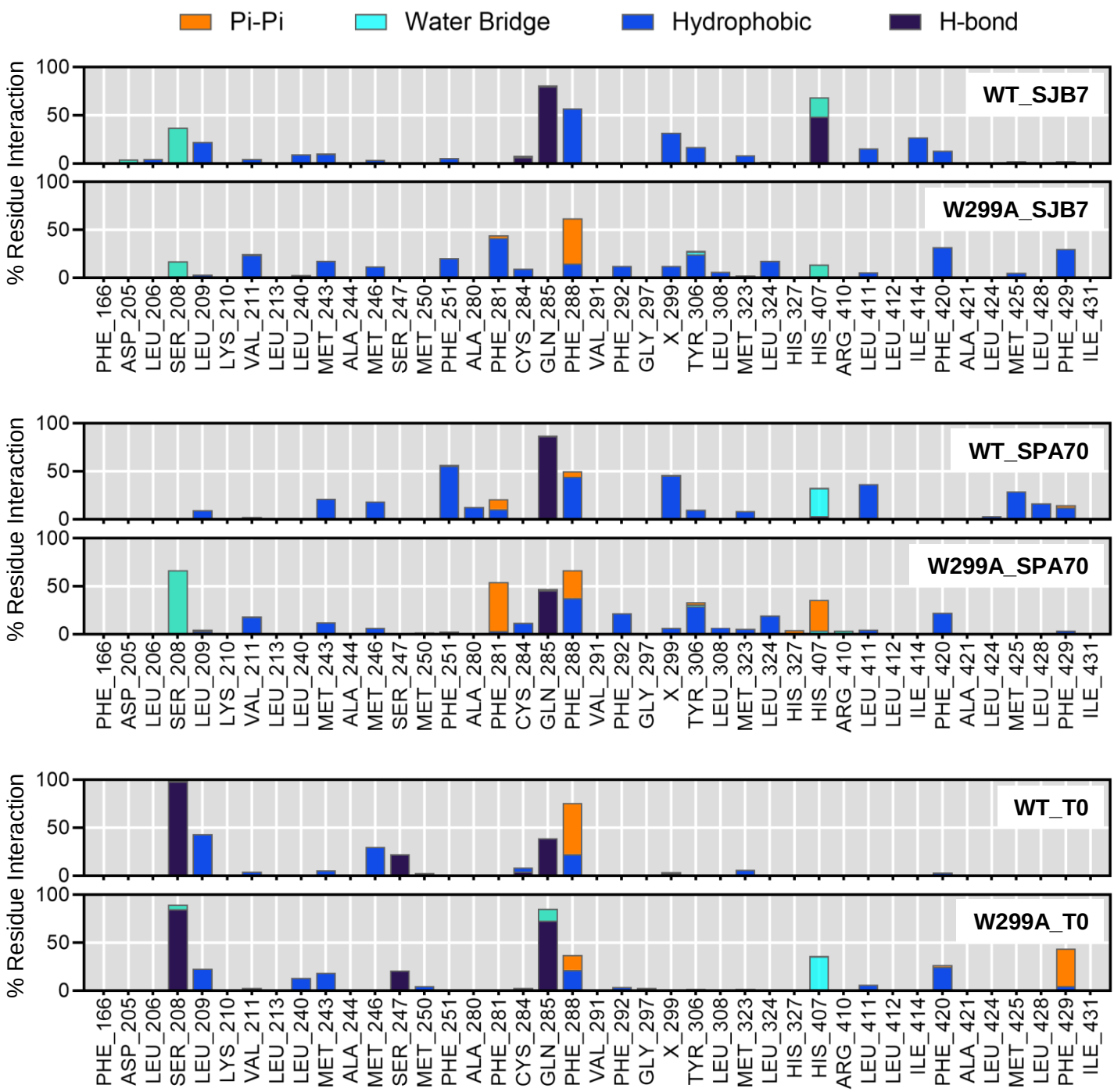

Supplementary Figure 16. Ligands have distinct interactions within the PXR ligand-binding pocket. Percentage residue interaction diagram demonstrating the residues interacting with the indicated ligands in WT or W299A PXR LBD. Only residues with ≥1% for at least one simulation course are shown.

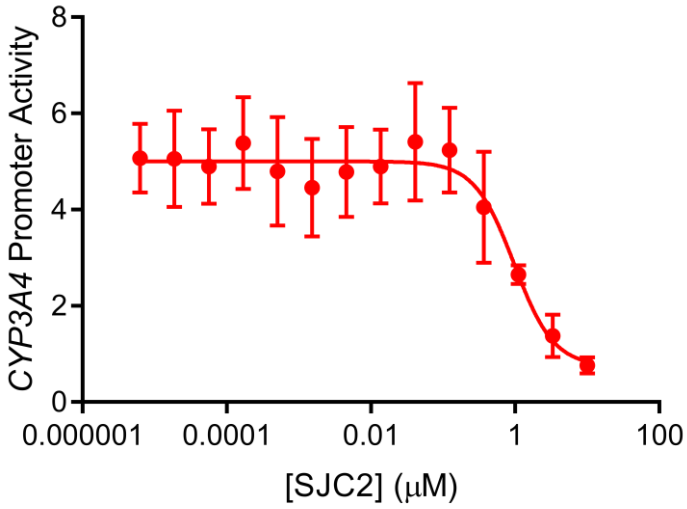

Supplementary Figure 17. SJC2 is an antagonist of WT PXR. HepG2 cells were co-transfected with WT PXR-expressing vector and a plasmid encoding firefly luciferase under the control of a PXR-responsive *CYP3A4* promoter. Cells were treated with the indicated concentrations of SJC2 in the presence of 10 μM Rif for 24 h and assayed for luciferase activity.

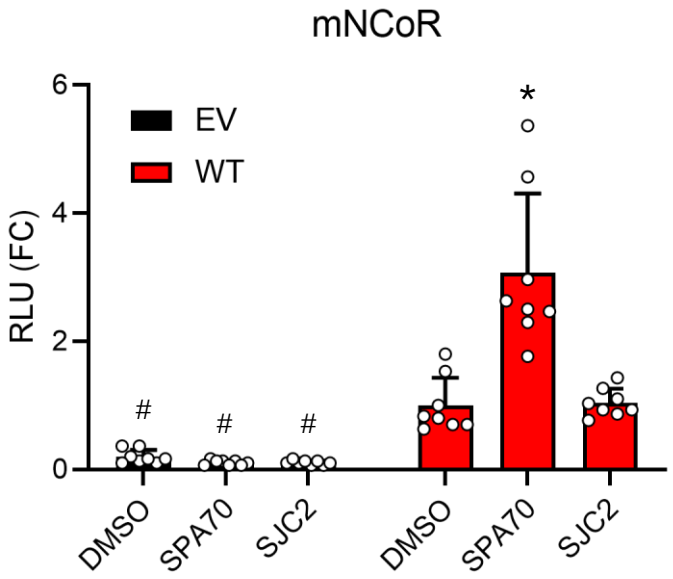

Supplementary Figure 18. SJC2 does not induce corepressor interaction with WT PXR LBD. Mammalian two-hybrid assays were performed in HepG2 cells. Cells were co-transfected with an empty pACT vector or pACT-PXR LBD plasmid, a coregulator plasmid (pBIND-mNCoR), and a GAL4 firefly luciferase reporter plasmid. Cells were treated with 10 µM SPA70 or SJC2 for 24 h and assayed for luciferase activity. The symbols represent measurements from 8 biological replicates. Data are presented as FC relative to the WT PXR DMSO control. Significance was assessed with one-way ANOVA followed by Dunnett's test for each sample compared to the DMSO control of its group [$p \leq 0.05$ (*)] and for each sample compared to the DMSO control for WT PXR LBD [$p \leq 0.05$ (#)].